CE 5315 Climate Science for Engineers

OPTION 2
for Project Work

-Stochastic Modeling of Weather Series in San Antonio Using an Advanced Weather Generator

- Pan Xinxin A0283981N

Background

San Antonio (SA) is a city in and the county seat of Bexar County, Texas, United States.
It has a greatest basketball team in NBA! Let’s focus on its climate!

Location in the United States

Climate

SA has a transitional humid subtropical climate that borders a semi-arid climate towards the west of the city featuring very hot, long, and humid summers and mild to cool winters. The area is subject to descending northern cold fronts in the winter and is warm and rainy in the spring and fall.

Precipitation & Temperature

SA is one of the most flood-prone regions in North America. July and August are the average warmest months, with an average high of 35 °C (seen in chart). The average coolest month is January. May, June, and October have quite a bit of precipitation.

Storm

Typically seeing snow, sleet, or freezing rain about once every two or three winters, but accumulation and snow itself are very rare. On January 13, 1985, it suffered a record snowfall of 41cm.
An F2 tornado lands within 80 km of the city on average once every five years.

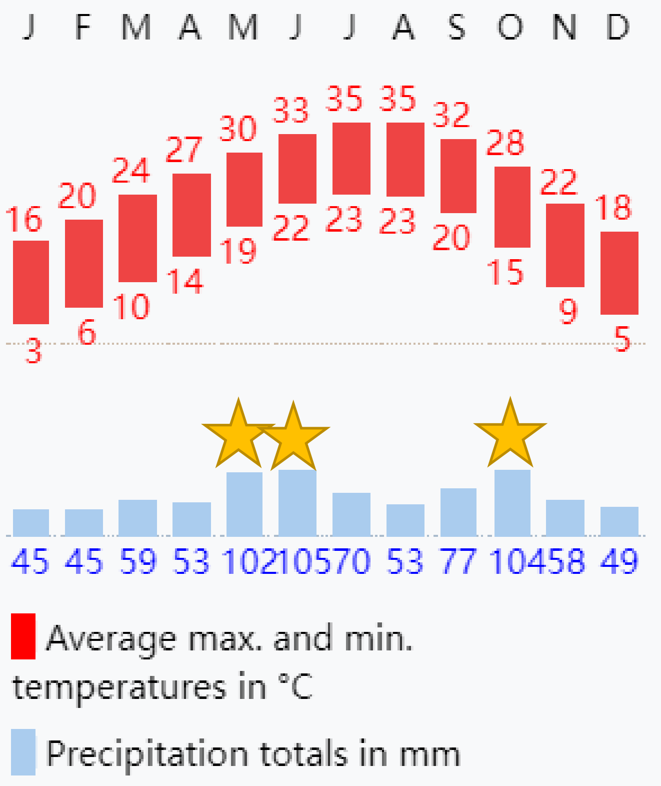

Fig.1. Climate chart in SA (Source: NOAA)

OPTION 2 for Project Work

Methodology

0. AWE-GEN & Statistical indicators
1. Precipitation
2. Cloud Cover Distribution
3. Air Temperature
4. Solar Radiation - Shortwave
5. Vapor Pressure
6. Wind Speed

Methodology ➢ AWE-GEN & Statistical indicators

AWE-GEN model

1. The AWE-GEN model has been successful in producing a broad range of temporal scale weather variables, ranging from the high frequency **hourly values** to the low-frequency inter-annual variability.
2. AWE-GEN with Gamma is used to generate 30 years of rainfall series at hourly scale in SA.
3. Neyman-Scott Rectangular Pulses (NSRP): the arrival times of storm origins occur in a **Poisson process** with rate λ where each storm origin generates a **random number C** of cell origins.
4. Autoregressive Lag-1 (AR1) model: it is employed to **preserve the variance and the autocorrelation** properties of the precipitation process at the annual scale.
5. To discuss the Seasonal Differences, a year is divided into **four seasons** as climatological patterns: December–January–February (DJF), March–April–May (MAM), June–July–August (JJA) and September–October–November (SON).
6. To obtain a stochastic ensemble, run AWE-GEN model with the weather data of SA station **21 times**, implying 21 versions of simulation results.

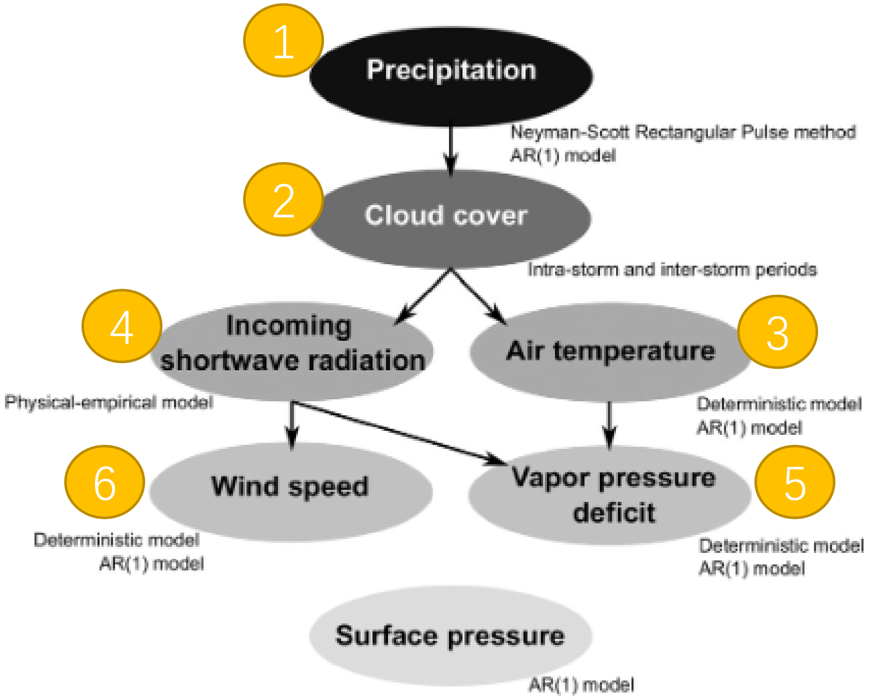

Fig.2 Schematic representation of the relationship between each simulated meteorological variable from the AWE-GEN model.

Statistical indicator:

1. Root Mean Square Error (RMSE): To evaluate the simulation performance of AWE-GEN: $RMSE = \sqrt{\frac{1}{n}\sum_{i=1}^{n}(y_i - \hat{y}_i)^2}$

Where *n* is the total number of data, y_i is the i-th observation rainfall amount and $\hat{y}_i$ is the simulation amount. Lower RMSE indicates smaller gap between the simulation and observation, and the model has a better performance.

Methodology

➢ 1 Precipitation

1. In AWE-GEN, the rainfall simulation is based on the **Poisson-cluster model**, whose reliability has been confirmed by a comparative analysis of its performance with numerous observed time series of precipitation.
2. Use statistical indicators to evaluate the precipitation distribution. If the value of simulation indictors **approximate to** that of observation, that indicates a good fitting results and trend.
3. To completely define the NSRP model, the parameters are estimated on a monthly basis considering the seasonality of site climatology, i.e., 6 parameters for each months need to be inferred.

Parameter	Explanation
λ^{-1}	Mean storm origin arrivals $[h]$
β^{-1}	Mean waiting time for cell origins after the origin of the storm $[h]$
η^{-1}	Mean duration of the cell $[h]$
μ_c	Mean number of cell per storm $[-]$
α	Shape parameter of the Gamma distribution of rainfall intensity $[-]$
θ	Scale parameter of the Gamma distribution of rainfall intensity $[mm\ h^{-1}]$

4. In model, there are 7 statistical indicators for precipitation analysis.

■ Statistical Indicators for Precipitation

Parameter	Meaning	Range	Evaluation of Data Distribution
Standard Deviations	Measure of the amount of variation or dispersion of data	$[0, \infty)$	Smaller values indicate less variability and tighter clustering of data around the mean, suggesting a more concentrated distribution. Larger values imply greater dispersion and a more spread-out distribution.
Mean	Represents the central tendency of the dataset	-	Ideally, the mean should be close to the center of the distribution, reflecting the typical value around which data points are clustered.
Variance	Measures the dispersion of data points around the mean	$[0, \infty)$	Smaller variance indicates data points tend to cluster around the mean, suggesting a more concentrated distribution. Larger variance implies more spread-out data.
Lag-1 Autocorrelation	Autocorrelation at a lag of 1, indicates linear relationship between adjacent time steps	[-1, 1]	Close to 1 indicates strong positive correlation, close to -1 indicates strong negative correlation. Close to 0 suggests relative independence between adjacent time steps.
Skewness	Measures the skewness of the data distribution	-	Positive skewness indicates right-skewed distribution, negative skewness indicates left-skewed distribution. Close to 0 suggests a relatively symmetric distribution.
Frequency of nonprecipitation	Frequency of events with no precipitation, proportion of time with no precipitation	[0, 1]	A lower frequency suggests less time with no precipitation, while a higher frequency implies more time without rainfall.
Transition probability wet-wet	Probability of transitioning from wet to wet state, probability of consecutive wet states	[0, 1]	High transition probability indicates persistence of wet conditions. A value close to 0 suggests less consecutive wet states, indicating more variability in wet and dry periods.

Methodology

➢ 2 Cloud Cover Distribution

1. In AWE-GEN model, some parameters for Cloud process are related to some **assumption**.

(1) The cloud cover can be assumed **stationary** and fully characterized by the first two statistical moments: the mean M0 and the variance.

(2) The second assumption is that **the transition of the cloud process** between the boundary of a storm period and the fair-weather takes place through an exponential function.

2. Other 2 parameters, acloud and bcloud, are from the **Beta distribution** that are used to generate random variates.
3. During an **intra-storm** period, i.e. the hours with precipitation>0, assume the value of cloudiness is equal to 1.
4. During an **inter-storm** period, the existence of the “fair weather” region is assumed.
5. Total Cloud Distribution fraction ranges [0,1], where 0 signifies **clear sky** conditions and 1 is used to describe **complete overcast** conditions (storm).
6. Cloud cover **N(t)** is the fraction of the celestial dome occupied by clouds. N(t) is considered to be a random variable that has different dynamics during intra-storm and inter-storm periods. In model, firstly, the threshold value Tr of the transition period is determined to **identify the fair-weather region**, i.e., the region where N (t) is stationary. That means the simulation results highly depends on the threshold value Tr.

■ Statistical Indicators for Cloud Process

Parameter	Explanation
M0	Mean fair weather cloudiness for cloud cover.
σ	Standard deviation fair weather cloudiness for cloud cover. Larger values imply greater dispersion and a more spread-out distribution
ρ	Lag-1 autocorrelation of mean fair weather cloudiness. Close to 1 indicates strong positive correlation, close to -1 indicates strong negative correlation.
γ	Cloudiness decay rate(h^{-1});
Tr	Length transition period (h); The length of the post-storm transition period after which the cloud cover process

$$N(t) = M_0 + (J_1 - M_0)(1 - J(t)) + m(t)J(t)$$

Methodology

➢ 3 Air Temperature

1. In AWE-GEN, the generation of air temperature, T(t) [℃], is simulated as the sum of a stochastic component, dT(t) and a deterministic component $\tilde{T}(t)$: $T(t) = \tilde{T}(t) + dT(t)$
2. The stochastic temperature component dT(t) is estimated through an autoregressive model AR(1). At the hourly scale, the random deviate of temperature exhibits a significant dependence in the hour of the day. That indicates in hourly timestep or scale, the difference between simulation and observation maybe obvious.
3. The stochastic component is particularly important for the determination of extreme of air temperature. Therefore, evaluate the model performance by focusing on the extreme temp.

■ Statistical Indicators for Air Temperature

Parameter	Explanation
B	Regression coefficients of deterministic component of temperature first order differential equation for air temperature
$\overline{dT_h}$	Mean random temperature deviate
ρ_{dT}	Lag-1 aoutocorrelation random temperature deviate
$\sigma_{dT,h}$	Standard deviation random temperature deviate
Ti	First step temperature(°C)

➢ 4 Solar Radiation - Shortwave

1. The main components for shortwave incoming radiation are direct and diffuse radiation.
2. Considering the **Julian Day**, obtain the correction factor E0 as a function of the daily angle. Thus, the extraterrestrial radiation, R'_0, can be obtained starting with the value of the solar constant R_0.

Total Shortwave Radiation: R_{sw}

$$R_{sw} = R_{dir} + R_{dif}$$

R_{dir}: direct radiation [W m-2]
R_{dif}: diffuse radiation [W m-2]

R_{dir} is directional, it depends on sun position (z) and needs to be projected on the surface of interest, R_{dif} is isotropic and is coming from all directions.

Methodology

➢ 4 Solar Radiation - Shortwave

3. For these 8 parameters in AWE-GEN, the ozone μ0 and the nitrogen dioxide μn have a minimal influence in the overall process. The surrounding ground albedo ρ_g depends on the location. In SA, a mostly snow-free region, its value is typically between 0.1 and 0.25.
4. These parameters, especially β, have a strong effect in determining the clear sky irradiance. Suitable values of α and β can be derived from the spectral irradiance measurement. β can vary several orders of magnitude reflecting sky conditions, from nearly zero (0.001 or less) for clear sky to 0.5 for very hazy conditions.
5. For overcast conditions, cloud cover fractions and the **cloud optical thickness** are used to described the radiative properties of clouds. In AWE-GEN, the process is simulated by liquid water path LWP, which is a property for cloudy sky condition and estimated from a reference value **LWP_R** [g/m^2].
6. In the model, only parameters **β** and **LWP_R** are generated by monthly.

■ **Statistical Indicators for Solar Radiation**

Parameter	Explanation
μ0	Ozone for solar radiation (cm)
μn	Nitrogen dioxide for solar radiation (cm)
α_A	Angstrom turbidity parameter for solar radiation
ω_A1	Single scattering albedos for solar radiation
ω_A2	
ρ_g	Surrounding ground albedo for solar radiation
LWP_R	The reference value of the liquid water path(g/m2)
β_A	Angstrom turbidity parameter for solar radiation

Methodology

➢ 5 Vapor Pressure

1. In order to simulate vapor pressure, a framework **similar to** the one used to model air temperature is proposed: Δe is simulated as the sum of the deterministic component, $\widehat{\Delta e}$ and the stochastic component, dΔe: $\Delta e(t) = \widehat{\Delta e}(t) + d\Delta e(t)$.
2. The ambient vapor pressure e_a is calculated as the difference between the vapor pressure at saturation e_{sat} and Δe(t).
3. The metrics of **air humidity** is evaluated by investigating several statistical properties of vapor pressure, e_a [Pa], relative humidity, U, and dew point temperature, T_{dew} [◦C].

■ Statistical Indicators for Vapor Pressure

Parameter	Explanation
a_Vap	Regression coefficients of deterministic component of vapor pressure
$\overline{d\Delta e}$	Average of vapor pressure deficit deviations
$\rho_{\Delta e}$	Lag-1 autocorrelation of the process
$\sigma_{\Delta e}$	Standard deviation of vapor pressure deficit deviations

➢ 6 Wind Speed

1. For wind speed , a framework **similar** is proposed: W_s is simulated as the sum of the deterministic component, $\widehat{W_s}$ and the stochastic component, dW_s: $W_s(t) = \widehat{W}_s(t) + dW_s(t)$
2. The deterministic component, $\widehat{W_s}(t)$, relates the wind speed to the incident global shortwave radiation, R_{sw}. Another factor affecting $\widehat{W_s}(t)$ is the parameter ci, that is estimated with **conventional regression techniques**.
3. As wind speed generally does not present marked differences throughout the year, therefore the parameters are derived and assumed to be valid for all months.

■ Statistical Indicators for Wind Speed

Parameter	Explanation
ci	Regression coefficients of deterministic component of wind speed
$\overline{dW_s}$	Average wind speed deviation
ρ_{dW_s}	Lag-1 autocorrelation of the process of wind speed
σ_{dW_s}	Standard deviation of wind speed
γ_{dW_s}	Skewness of wind speed

Results and Analysis

1. Precipitation
2. Cloud Cover Distribution
3. Air Temperature
4. Solar Radiation - Shortwave
5. Vapor Pressure
6. Wind Speed

Results and Analysis

➢ 1 Precipitation

➢ Parameter and results analysis

1. For the same value of **λ** close to 0.01 as storm origin arrivals in SA expect in July and August. A lower λ means the estimated storm origin arrival rate is lower and on average there are fewer new storms per unit time.
2. **β** means waiting time for cell origins after the origin of the storm. During JJA, relatively lower λ and β may result in storm events that are more discrete and occur less frequently.
3. **μc** means number of cell per storm and **η** indicates the duration time of cell. During SON, μc and η is higher, indicating the rainfall activity is heavier during this season.
4. **α** and **θ** shows the shape and scale of rainfall intensity. Generally, a lower α implies the smaller probability of the occurrence of rainfall extremes.

- Estimated NSRP parameters of AWE-GEN with Gamma Distribution

	λ	β	μc	η	α	θ
Jan	0.009	0.37	6.57	0.86	0.10	8.55
Feb	0.006	0.07	9.77	1.73	0.40	5.20
Mar	0.006	0.06	2.31	2.33	1.64	4.96
Apr	0.007	0.11	3.02	3.65	0.91	15.80
May	0.008	**0.02**	1.68	1.38	1.81	8.39
Jun	0.007	0.16	3.29	3.11	1.22	16.01
Jul	**0.003**	0.05	3.83	2.11	1.23	11.83
Aug	**0.004**	0.04	2.92	2.16	1.82	9.58
Sep	0.007	0.17	15.02	1.79	0.11	18.38
Oct	0.007	0.12	2.88	2.30	1.06	10.99
Nov	0.006	0.22	**25.27**	**3.92**	0.10	23.65
Dec	0.009	**0.85**	1.26	1.13	0.97	5.15

Note: Range: $0.0001 < \lambda < 0.05$; $0.01 < \beta < 0.99$; $1 < \mu c < 80$; $0.5 < \eta < 30$; $0.1 < \alpha < 20$.

- ☐ It should be noted that these parameters determine the simulation results. If there is an obvious gap between simulation and some of parameters' indicators, that can be explained as these types of parameter do not give high contribution to the rainfall activity.

Results and Analysis

➢ **1 Precipitation:** **Parameter and results analysis**

➢ Verify the effect on rainfall events by parameters

1. Visualize the rainfall intensity in 30-year period(Seen in Fig.3.1), and choose the series in **1963** as well distribution and without extreme rainfall.
2. Use RMSE to compare 21 times simulation results(Seen in Fig.3.2) and choose Verison6(RMSE=1.05 close to 1) as the better simulation to read rainfall events in 1963 by hourly (Seen in Fig.3.4). But the model performance show the "overdispersion" issue due to the nonconcentrated distribution of simulation rainfall.
3. It can be seen that in Nov, with higher μc and η, the total rainfall amount is greater than other months'. And with a relatively high λ and β during SON, the rainfall distribution is concentrated and continuous, and the time intervals is shorter.
4. For the rainfall extremes, although the shape parameter α keeps higher during JJA, it causes the highest intensity in Aug.
5. However, the highest scale parameter θ is observed in Dec, the simulation does not show the same trend, implying the scale parameter has a more pronounced impact on extreme rainfall activity compared to the shape parameter α.

Fig.3.1 Pr_obs in SA

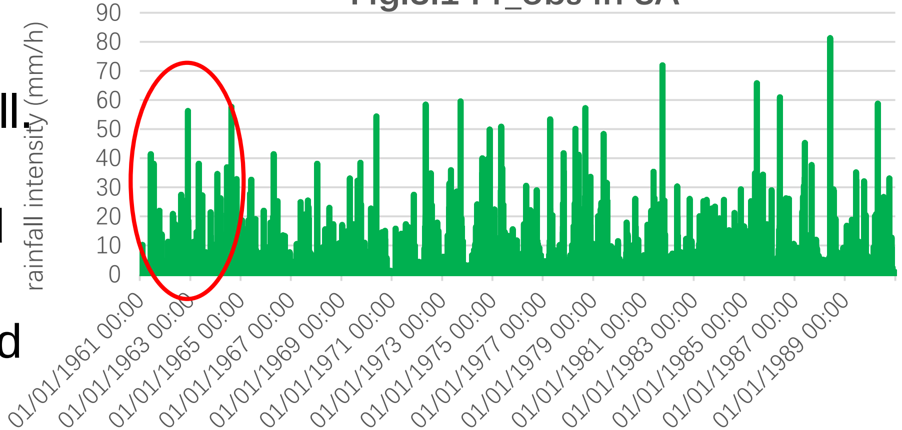

Fig.3.2

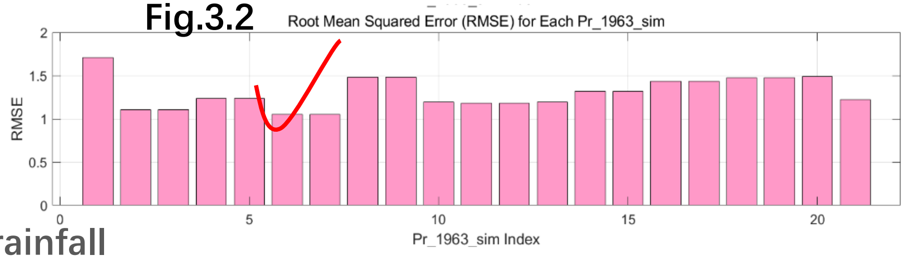

Fig.3.4 Comparison hourly data of rainfall

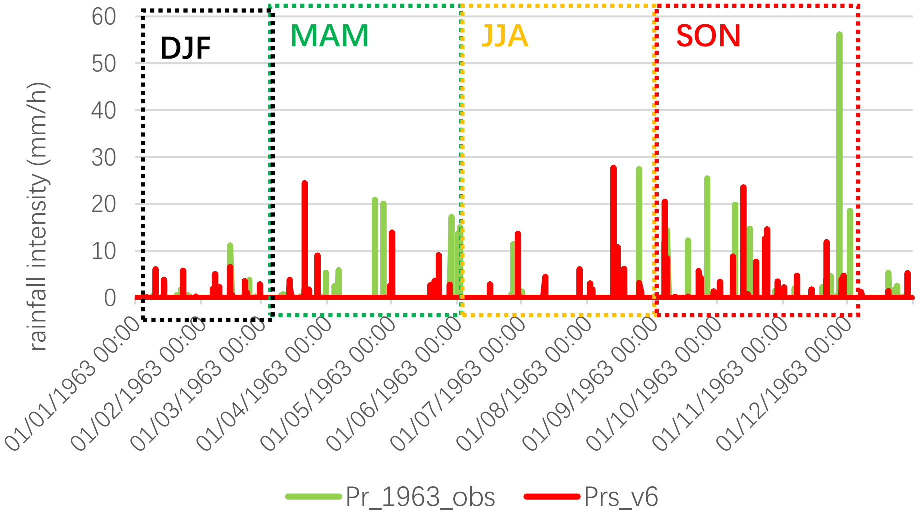

Fig.3.3 Parameter for Precipitation

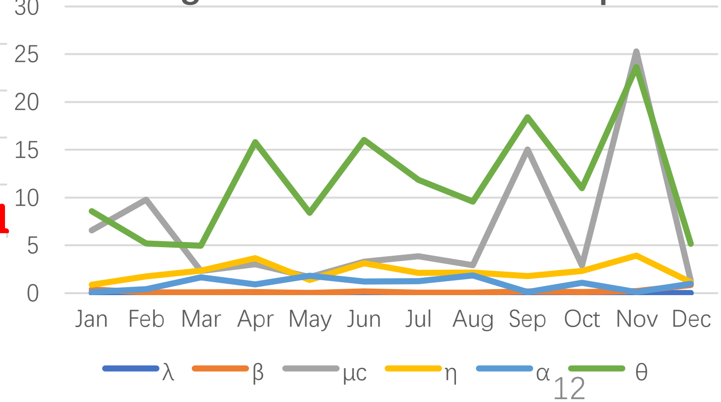

Results and Analysis

1 Precipitation

Monthly statistics of precipitation

1. Although parameters give high contribution to the rainfall activity in 1963, the fitting condition hourly is **not satisfying**. To take into account the seasonality of site climatology, the analysis results are computed monthly in AWE-GEN.
2. To evaluate the fitting condition by **monthly statistics**, Fig.3.5 shows that a good fitting occurs in February and October, as the smaller standard deviation representing better model performance.
3. In Fig.3.6 for 1hr aggregation period, these 6 indicators well simulated to assess the similarity between distributions of simulation and observation, it is evident that the better performance occurs in SON seasonally.
4. Considering the parameters in SON, the variance (from 2.18 to 0.89) shows a more concentrated distribution in rainfall intensity about 0.13 to 0.08mm/h, satisfying with the climate in SA that October generally has quite a bit of precipitation.
5. In August, a high value of Frequency of nonprecipitation indicates infrequent rainfall within wet season JJA, while a low value of Transition probability wet-wet signifies a low frequency of rainfall.

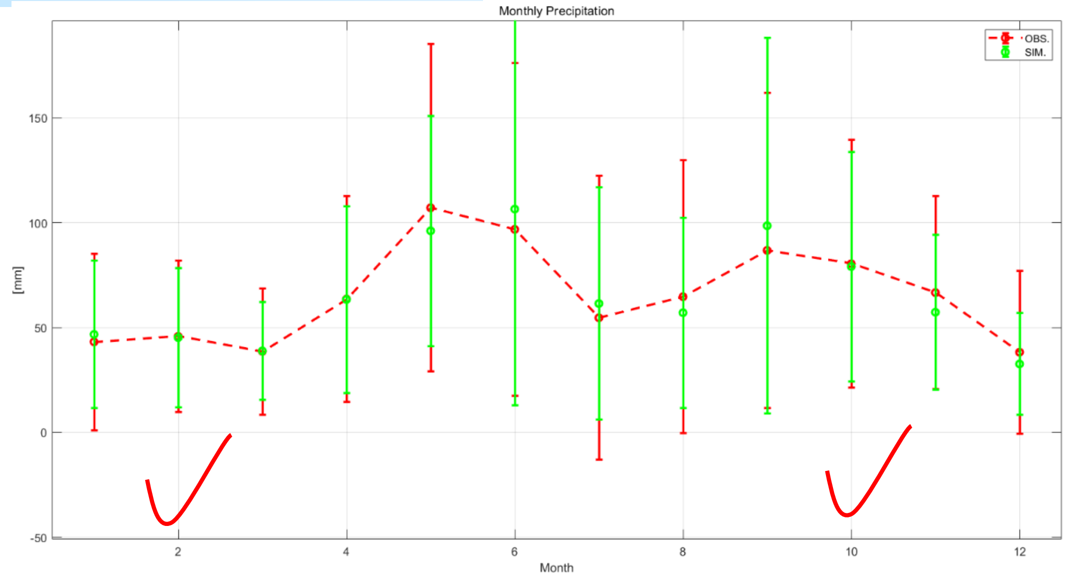

Fig.3.5 The standard deviations of the monthly precipitation

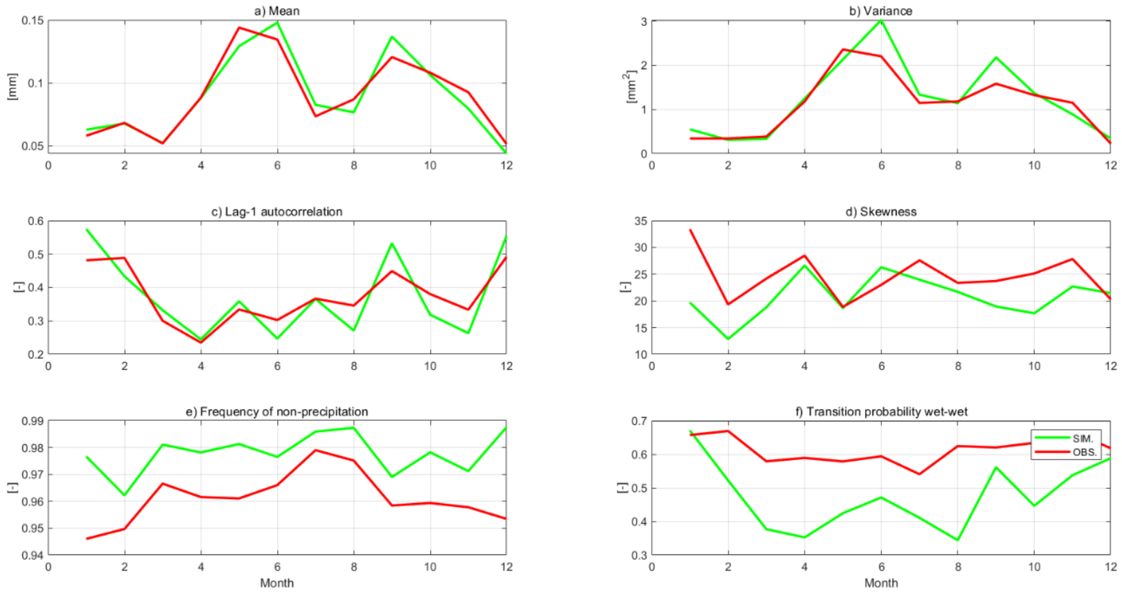

Fig.3.6 Comparison between observed (red) and simulated (green) monthly statistics of rainfall of **1 hour** aggregation period

Results and Analysis

➢ 1 Precipitation

➢ Different aggregation period in Monthly statistics of precipitation

1. With increasing aggregation period, the mean does not change, but the Lag-1 Autocorrelation becomes approaching to 0, indicating that larger aggregation period leads to increasing independence of rainfall data between adjacent time steps.
2. For **24hrs** aggregation period, the variance, lag-1 autocorrelation and skewness are well simulated, so that it can be chosen as the better aggregation period to analyse, and also reduce the computation and simplify the amount of data.
3. For **dry season** DJF, with increasing aggregation period, the simulation Transition probability wet-wet deviates more from the observation value. However, for the **wet season** JJA, especially in August with a low frequency of rainfall, the fitting performance improves.

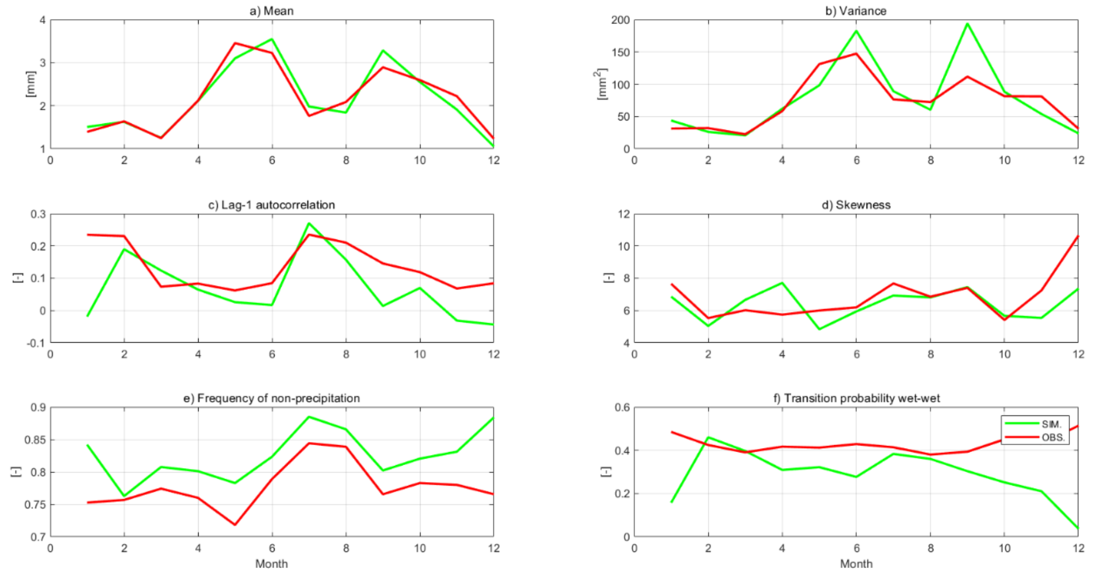

Fig.3.7 Comparison monthly statistics of **24hr** aggregation period

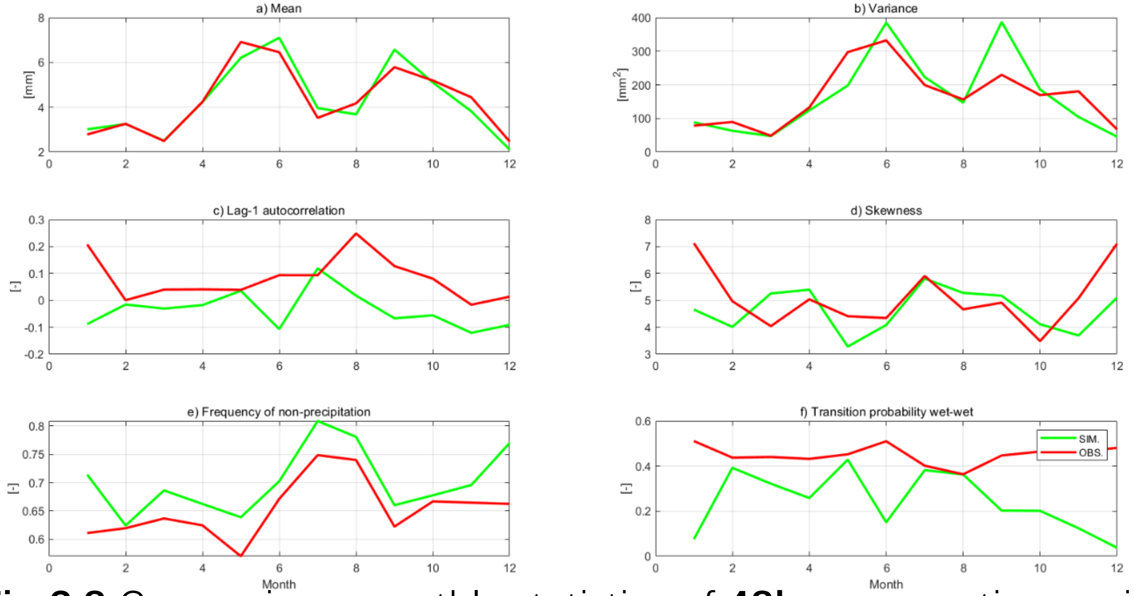

Fig.3.8 Comparison monthly statistics of **48hr** aggregation period

Results and Analysis

➢ 1 Precipitation

➢ Evaluate the frequency of non-precipitation and the transition probability for dry/wet situation

1. For the consecutive days, $E_{dry} = E_{obs} - E_{sim} = 7.95 - 7.85 = 0.1(\text{day})$, $E_{wet} = 1.55 - 1.33 = 0.22(\text{day})$. That means the mean of dry or wet consecutive days is underestimated.
2. Compared to the wet interval, the mean of dry interval is underestimated to a lesser degree.
3. The standard deviation of dry interval is obviously higher, suggesting greater variability or dispersion. That means it is **more difficult** to capture the accuracy of dry consecutive days in SA by model.

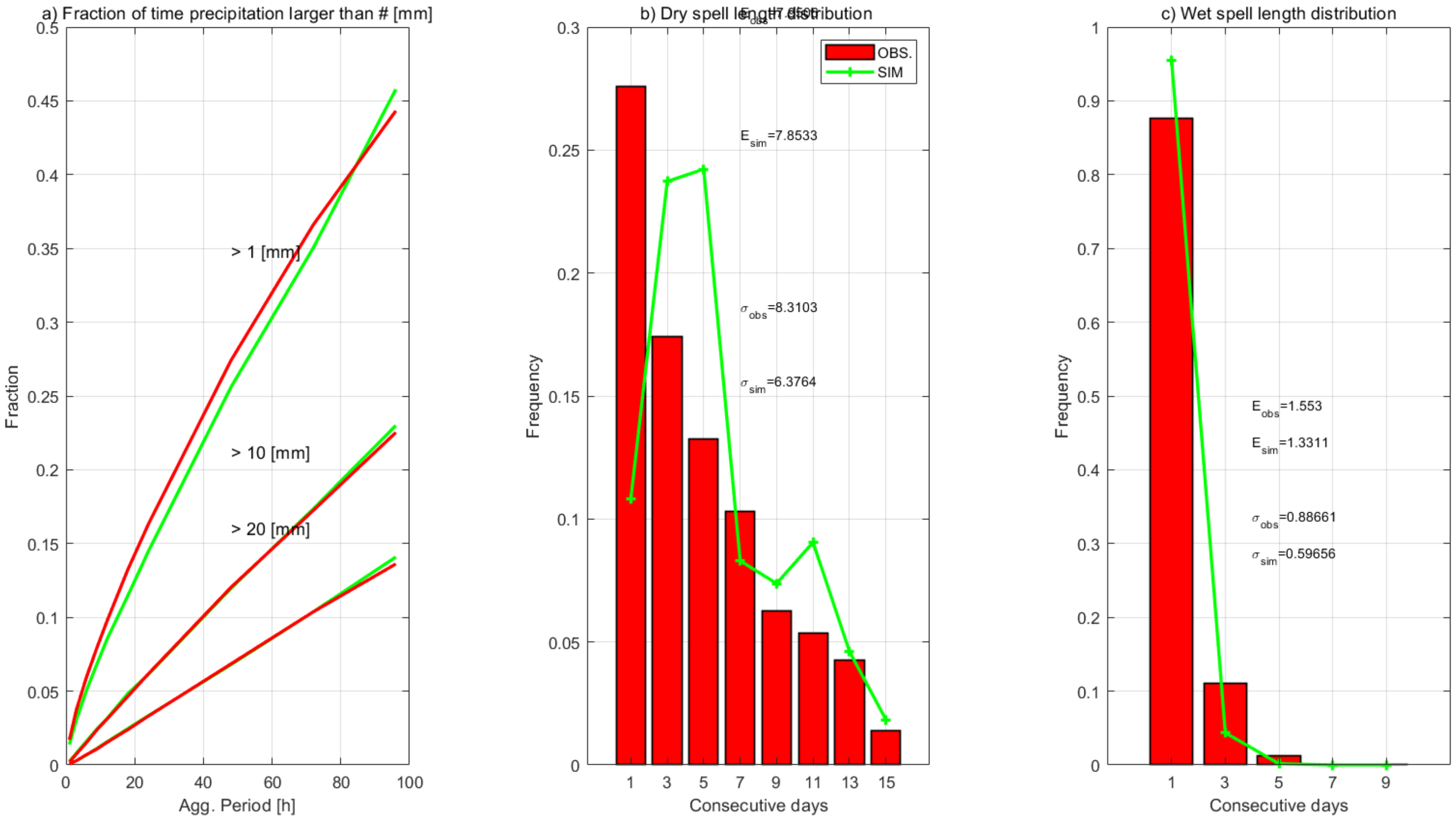

Fig.3.9 Comparison between observed (red) and simulated (green) of fraction of time, for dry interval length (a) The same comparison for dry spell length distribution; (b) consecutive days with precipitation depth lower than 1 [mm] and for wet interval length distribution; (c) consecutive days with precipitation depth larger than 1 [mm]. Note: **E and σ** are the mean and standard deviation.

Results and Analysis

➢ 1 Precipitation

➢ Evaluate the frequency of non-precipitation and the transition probability for dry/wet situation

1. The here is a considerable overlap between the simulated and observed extreme precipitation, up to the return periods of 10~20 years. For longer aggregation periods, it shows a better fitting results.
2. However, the hourly extreme precipitation is somewhat underestimated. Especially for the dry spell duration within a shorter return period less than 10 years, it is underestimated to a higher degree.
3. Extreme values of dry intervals in SA are poorly captured by the model.

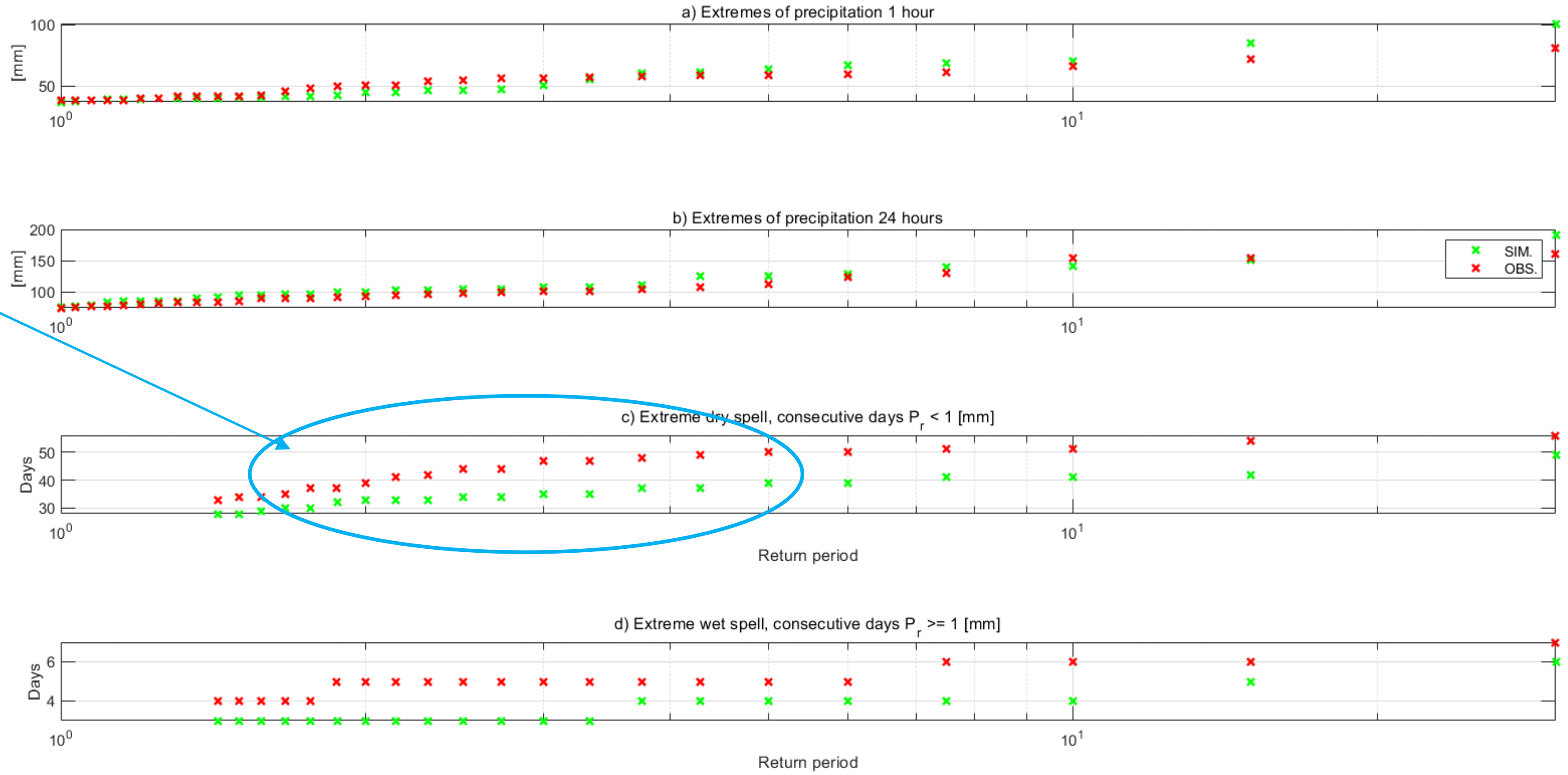

Fig.3.10 Comparison of extreme precipitation (green crosses) at (a) 1-hour and (b) 24-hour aggregation periods; (c) extremes of dry and (d) wet spell durations. Dry/wet spell duration is the number of consecutive days with precipitation depth lower/larger than 1 [mm]

Results and Analysis

➢ 2 Cloud Cover Distribution

➢ Parameter and results analysis

1. As the key point to simulate the cloud process is to identify fair-weather region, compare to the standard deviation of fair weather cloud cover distribution, and then choose Version12 as a better fitting version.
2. The model easily overestimates the simulation of fair weather but exhibits a strong capability in capturing storm conditions for total cloud cover distribution, as in overcast conditions it mostly aligns with observed values.
3. Considering the basic fair weather cloudiness (M0) as the basic term in N(t), and the smaller standard deviation σ and ρ being farther away from 1 indicates that the cloud distribution is more concentrating, thus there is less uncertainty for storm.
4. In Fig.4.1, as the fraction of N(t)=1 is the obvious gap between April(more storm), June and August, with decreasing M0 and σ and a weaker positive correlation, the less cloud cover leading to storm.

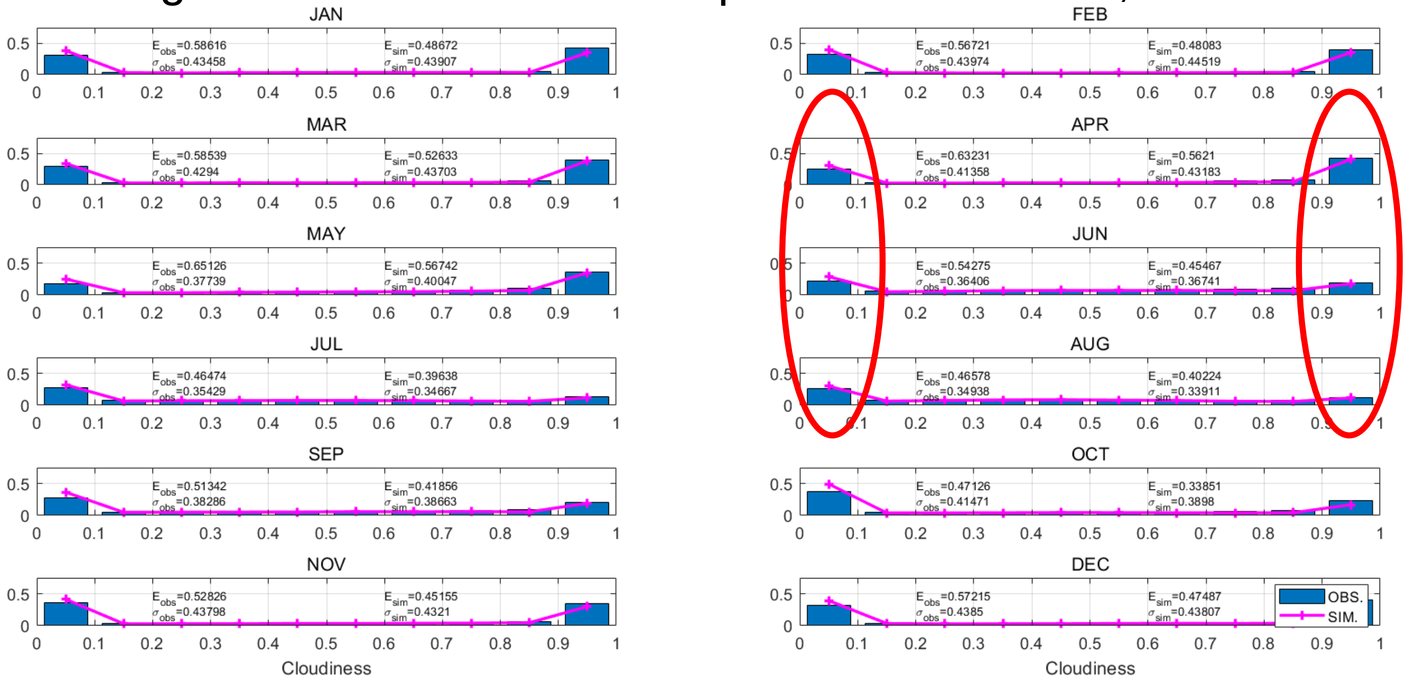

Fig.4.1 Comparison between the observed (cyan) and simulated (magenta) total cloud cover distribution

- Estimated cloud parameters of AWE-GEN

	M0	σ	ρ	γ	Tr
Jan	0.401	0.421	0.934	0.061	75
Feb	0.417	0.425	0.937	0.105	44
Mar	**0.479**	0.429	0.932	0.118	39
Apr	**0.516**	0.428	0.927	0.110	42
May	**0.513**	0.396	0.897	0.072	64
Jun	0.430	**0.360**	0.908	0.078	59
Jul	0.356	**0.326**	0.870	0.077	60
Aug	0.373	**0.319**	0.870	0.105	44
Sep	0.346	0.353	0.908	0.076	61
Oct	0.249	0.340	0.925	0.040	**115**
Nov	0.377	0.411	0.933	0.102	45
Dec	0.409	0.423	0.938	0.082	56

Results and Analysis

➢ 2 Cloud Cover Distribution

➢ Parameter and results analysis

1. For the performance, simulating the fair-weather period(Fig.4.2) is **more satisfying** than the one obtained for the total cloud cover(Fig.4.1), because the standard deviation σ of monthly distribution in the fair-weather period is closer to the observation (Seen in Fig.4.3).

Fig.4.3 Comparison of Standard deviation

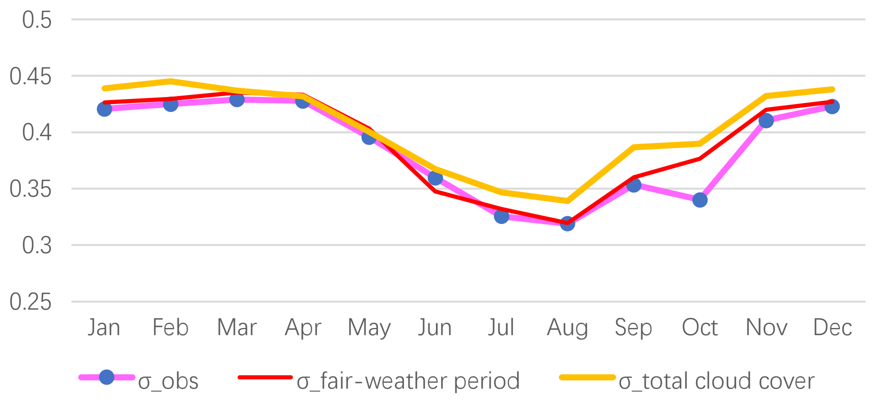

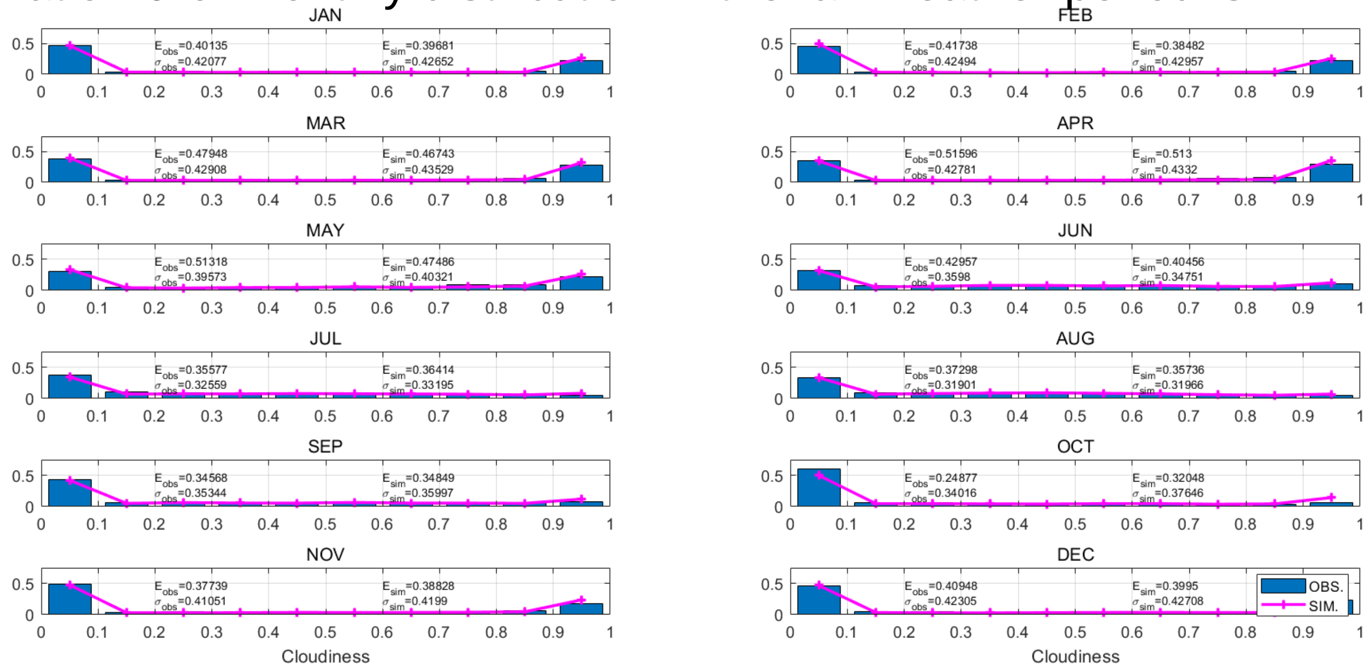

Fig.4.2 Comparison of fair weather cloud cover distribution.

2. Fig.4.3 shows during JJA, the performance is better, as the simulation trend almost coincides with that of observation.
3. In Fig.4.4, it can be seen that the easily overestimates the simulation of fair weather and underestimate the storm conditions in terms of cloud cover.

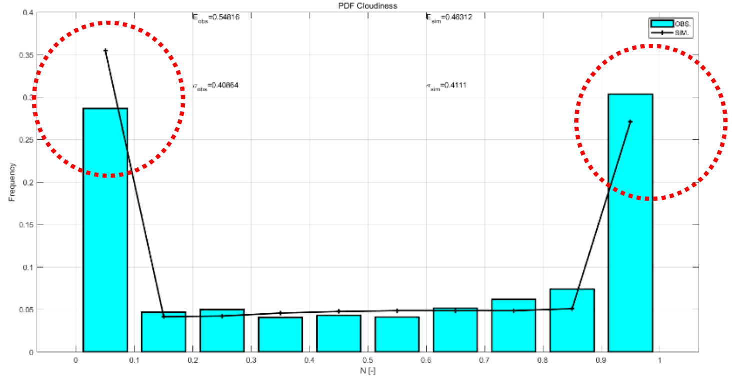

Fig.4.4 Comparison of total cloud cover distribution.

Results and Analysis

➢ 3 Air Temperature

➢ Parameter and results analysis

1. With the longer aggregation periods, the mean of monthly air temperature does not change, which shows a positive correlation with Ti (Seen in Fig.5.3). And the standard deviation σ within agg.period 24hrs is smaller, that shows a better performance.
2. For the capability to reproduce the distribution of monthly extreme temperature, the similar better performance is shown in the higher min or max of temp, but worse one in lower temp.
3. In terms of the mean, min and max of temperature, these indicators show the cross-correlation structure for air temperature that is inherent in AWE-GEN model closely matches that of the observation data(reality), which indicates a better model performance.

Fig.5.3 Parameters

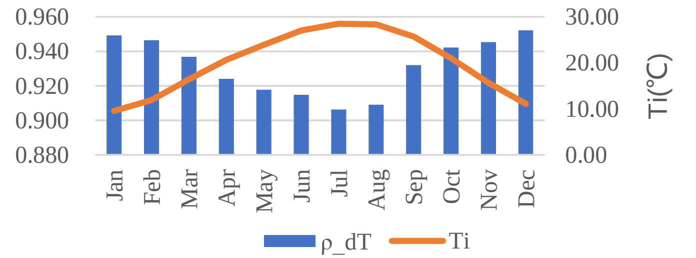

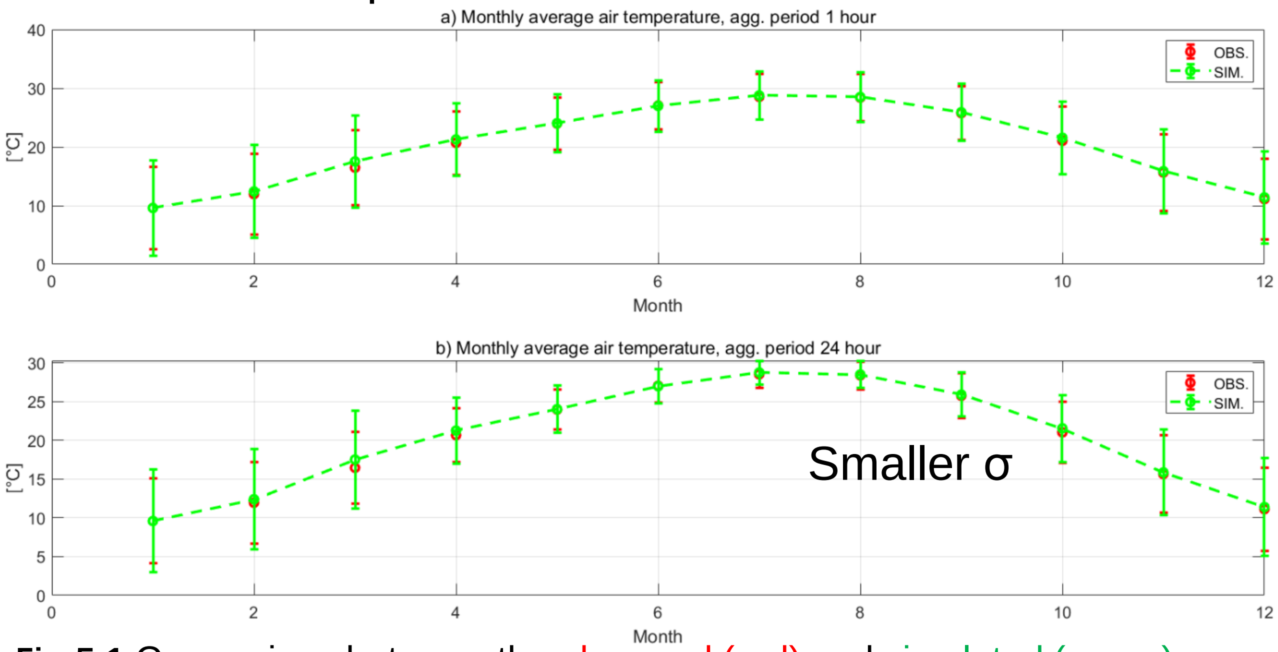

Fig.5.1 Comparison between the observed (red) and simulated (green) average air temperature for every month, aggregation periods of 1hr and 24hrs

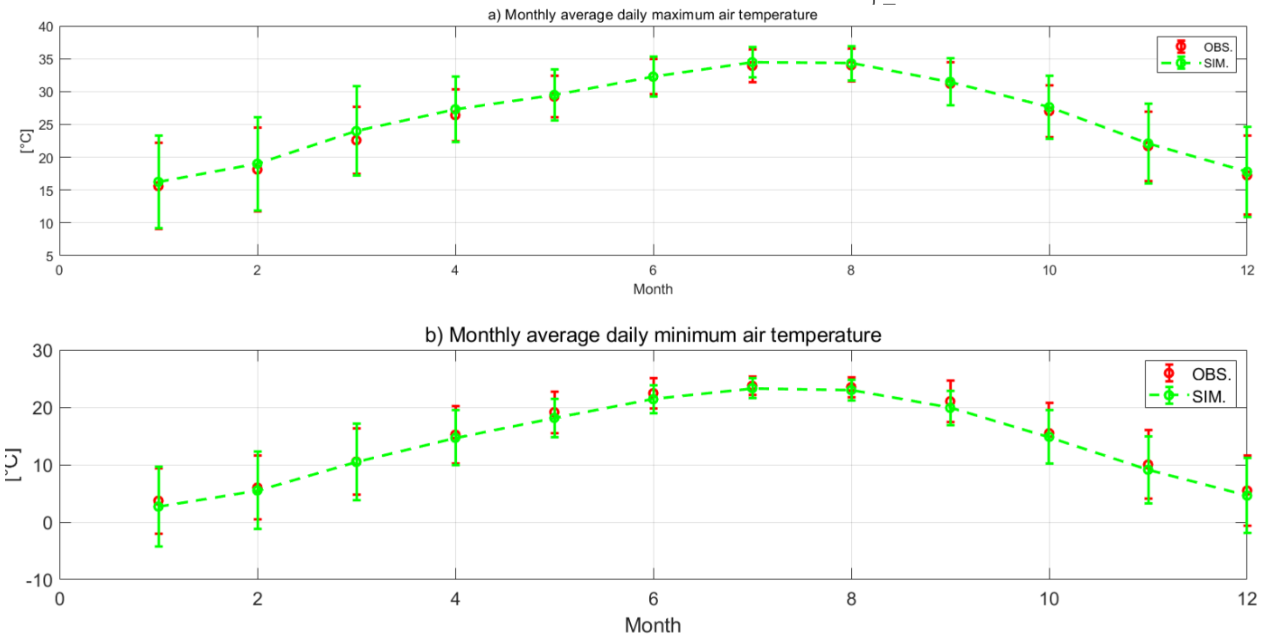

Fig.5.2 Comparison between the observed (red) and simulated (green) daily maximum (a) and minimum (b) air temperature for every month

Results and Analysis

➢ 3 Air Temperature

➢ Results analysis

1. In Fig.5.3a, it can be seen that the better performance occurs in the extreme air temperature, such as lower than -10 ℃ and greater than 40 ℃, but for the normal air temperature ranging 20~34℃, it shows the obvious gap between simulation and observation, implying a worse performance.
2. Further discussion of the extreme air temperature shown in Fig.5.4. Generally, within agg.period 24hrs, the min or max simulation temp matches better with the observation during shorter return period, that seems the longer agg.periods can eliminate model mismatch issues caused by short time steps(1hr).

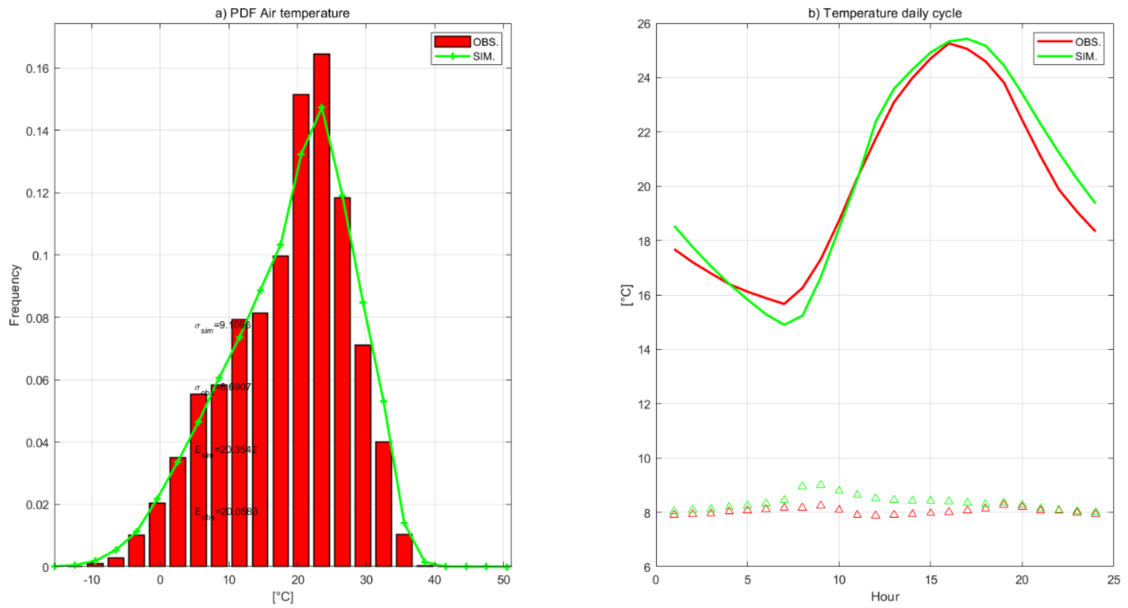

Fig.5.3a) Comparison between the observed (red) and simulated (green) air temperature distribution (a) and average daily cycle (b). **Fig 5.3b)** The triangles are the standard deviations for every day hour.

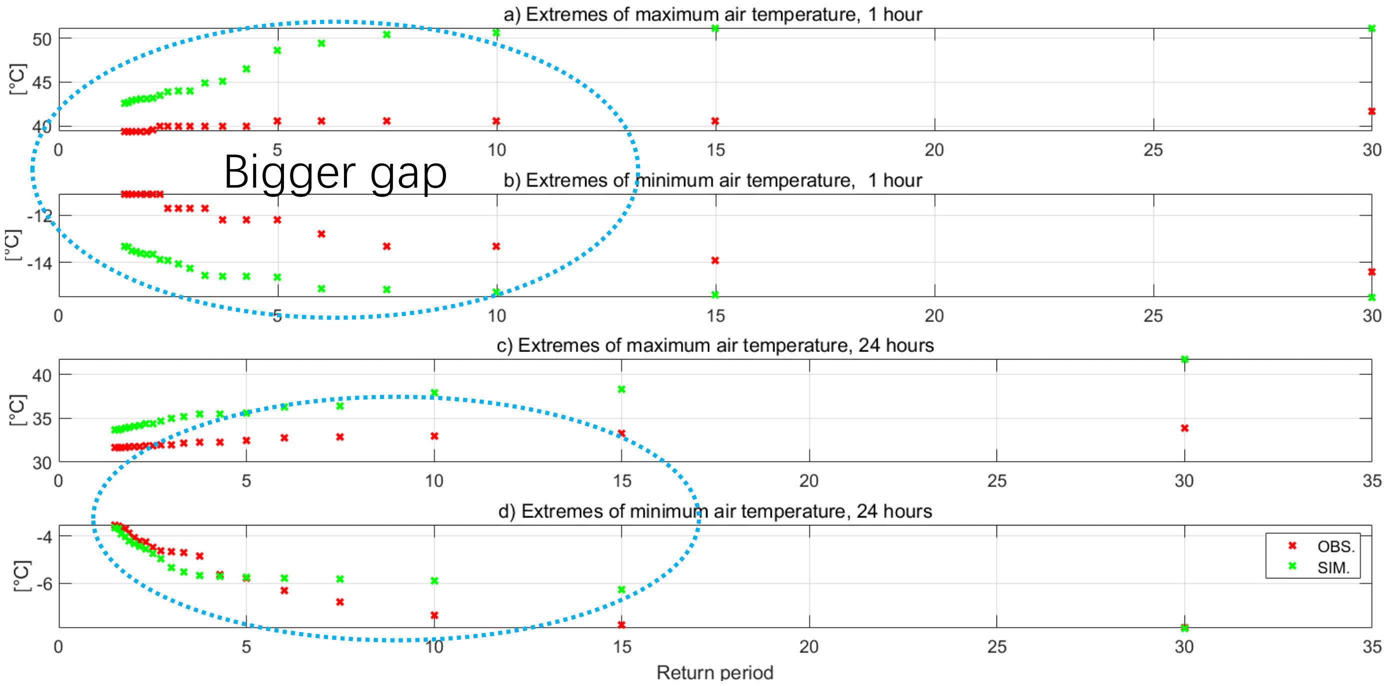

Fig.5.4 Comparison between the observed (red) and simulated (green) extremes of air temperature. a) Maxima of hourly temperature. b) Minima of hourly temperature. c) Maxima of daily temperature. d) Minima of daily temperature.

➢ Parameter and results analysis

1. Considering the total cloud cover distribution in Fig.4.1, during JJA the fair-weather conditions dominates. Therefore, the global shortwave radiation within JJA is higher.
2. Meanwhile, Fig.4.2 shows the better performance of cloud distribution occurs in JJA, and combination of Fig.6.1, the gap of mean and σ is smaller in JJA, also implying a better performance of global shortwave radiation. That can verify the **positive correlation of simulation between cloud and shortwave radiation**.
3. As LWP_R is used to described cloud optical thickness relating to the fair-weather and shortwave radiation, the lower LWP_R in JJA causes higher shortwave radiation, implying the smaller cloud thickness.
4. β also determines the clear sky irradiance, and in JJA, β is higher.

- Shortwave radiation parameters

	μ0	μn	α_A	ω_A1	ω_A2	ρ_g	LWP_R	β_A
Jan	0.35	2.00E-04	1.30	0.920	0.840	0.150	65.85	0.022
Feb							57.43	0.025
Mar							47.56	0.043
Apr							42.96	0.056
May							39.58	0.073
Jun							**37.55**	**0.068**
Jul							**35.17**	**0.068**
Aug							**20.51**	**0.069**
Sep							39.80	0.043
Oct							48.37	0.025
Nov							58.54	0.019
Dec							65.62	0.020

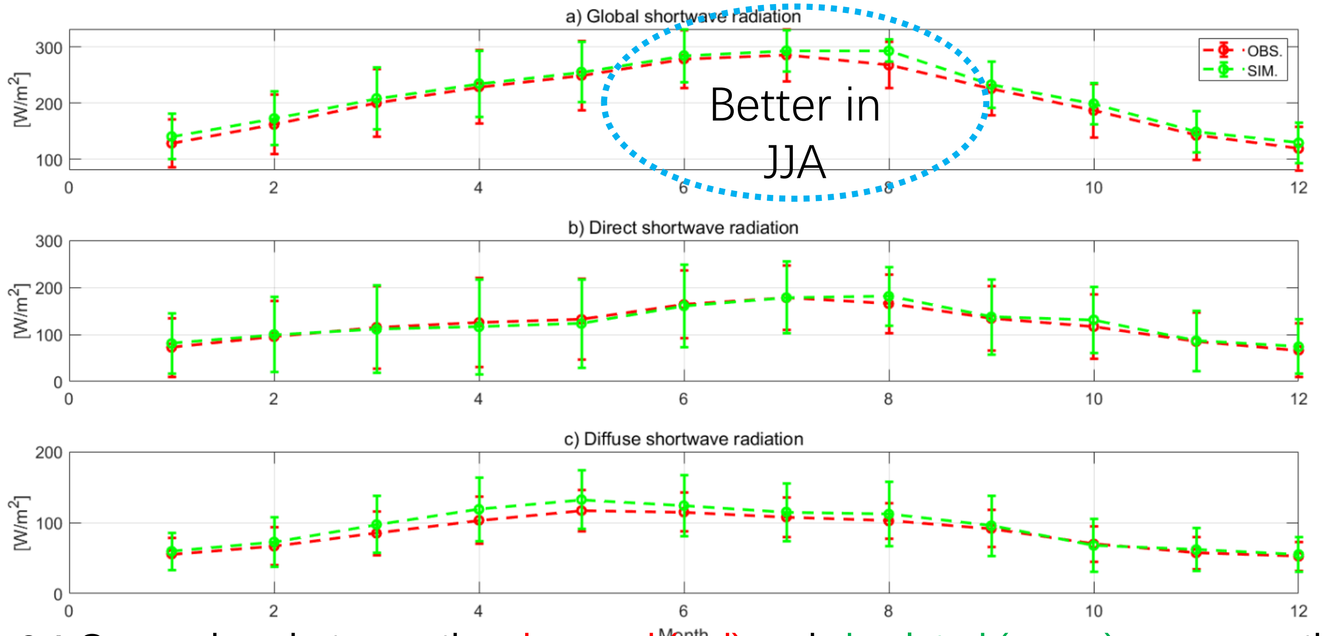

Fig.6.1 Comparison between the observed (red) and simulated (green) mean monthly shortwave radiation. a) Global radiation. b) Direct beam radiation. c) Diffuse radiation.

➢ Parameter and results analysis

1. By combination of Fig.6.1 and Fig.6.2, AWE-GEN tends to overestimate direct radiation and underestimate diffuse radiation to a higher degree, thus the global shortwave radiation is obviously overestimated.
2. Focusing on the sunrise (8:00-9:00) and sunset (18:00-19:00) hours in a day(Seen in Fig.6.3), the model performs worse. This discrepancy might be attributed to the reflection of beam radiation causing radiative fluxes before sunrise and after sunset or potential measurement errors that are more likely to occur under low radiation density.

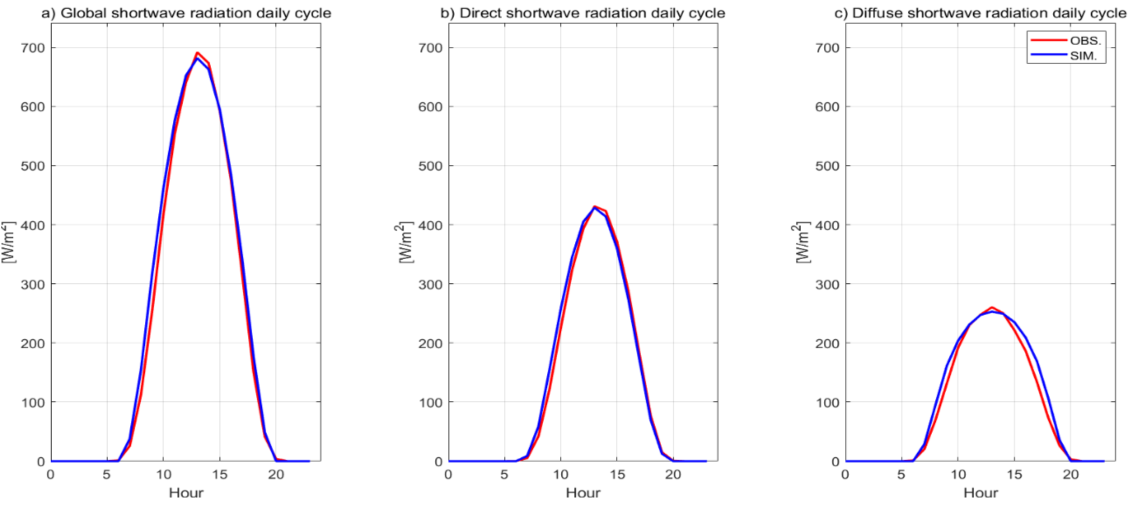

Fig.6.2 Comparison between the observed (red) and simulated (blue) daily cycle of global (a), direct (b) and diffuse (c) shortwave radiation.

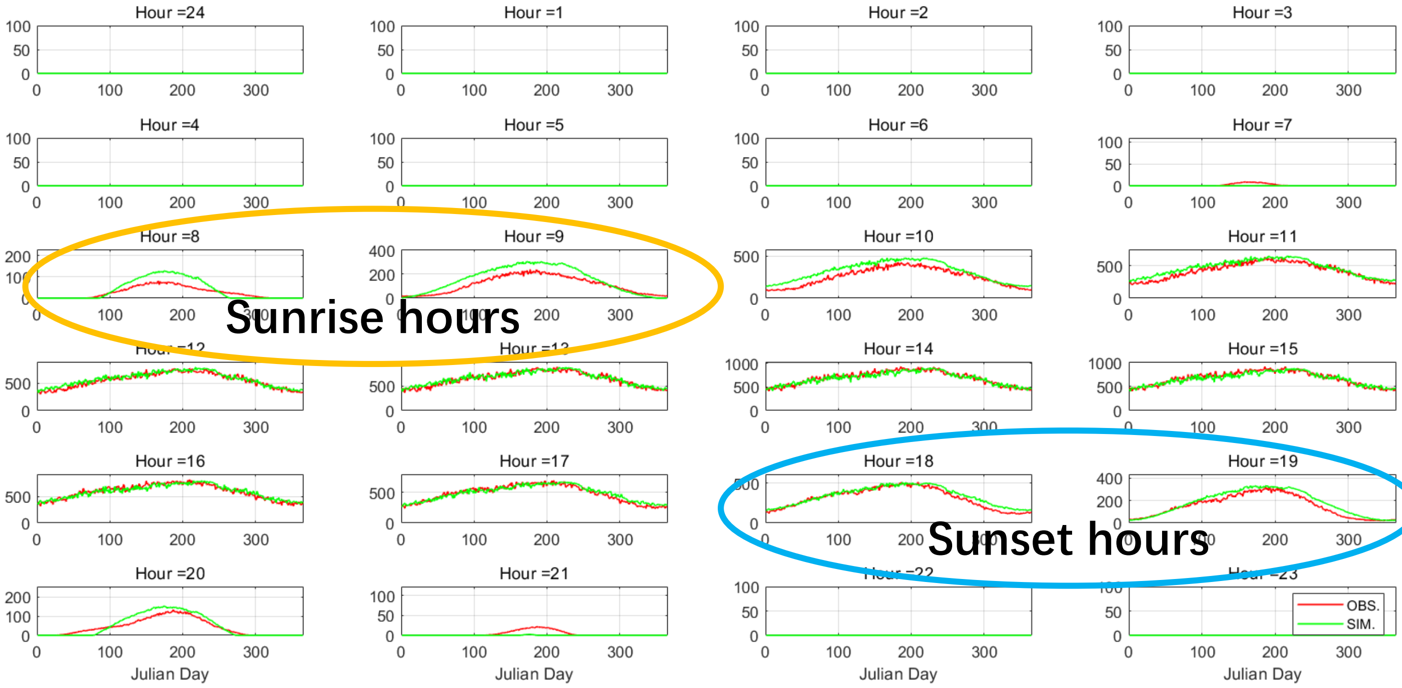

Fig.6.3 Comparison between the observed (red) and simulated (green) annual cycle of global shortwave radiation for different local time hours. The global shortwave fluxes are expressed in [W/m2]

Results and Analysis

➢ 5 Vapor Pressure

- Vapor Pressure parameters

	$\overline{d\Delta e}$	$\rho_{\Delta e}$	$\sigma_{\Delta e}$
Jan	4.05E-14	0.953	272.894
Feb	-1.59E-13	0.949	300.695
Mar	-2.93E-13	0.947	379.790
Apr	-4.65E-13	0.940	421.557
May	-1.89E-01	0.936	379.891
Jun	-2.51E+00	0.930	312.205
Jul	-1.40E+00	0.927	265.016
Aug	-1.89E+00	0.927	277.814
Sep	-3.63E-01	0.935	401.777
Oct	1.50E-13	0.924	361.200
Nov	-2.00E-13	0.933	304.404
Dec	1.62E-13	0.943	270.149

➢ Parameter and results analysis

1. Similar to other discussion of agg period, the different agg periods cannot affect the mean relative humidity and vapor pressure (Seen in Fig.7.1~7.2). And its change can be captured well based on a small gap of σ, but for 24hrs, the model generally underestimates its variance and the gap of σ is increasing.
2. For U<60% defined as relatively dry weather, the model performance in wet weather is better than that in dry climates. Overall the performance is quite remarkable.

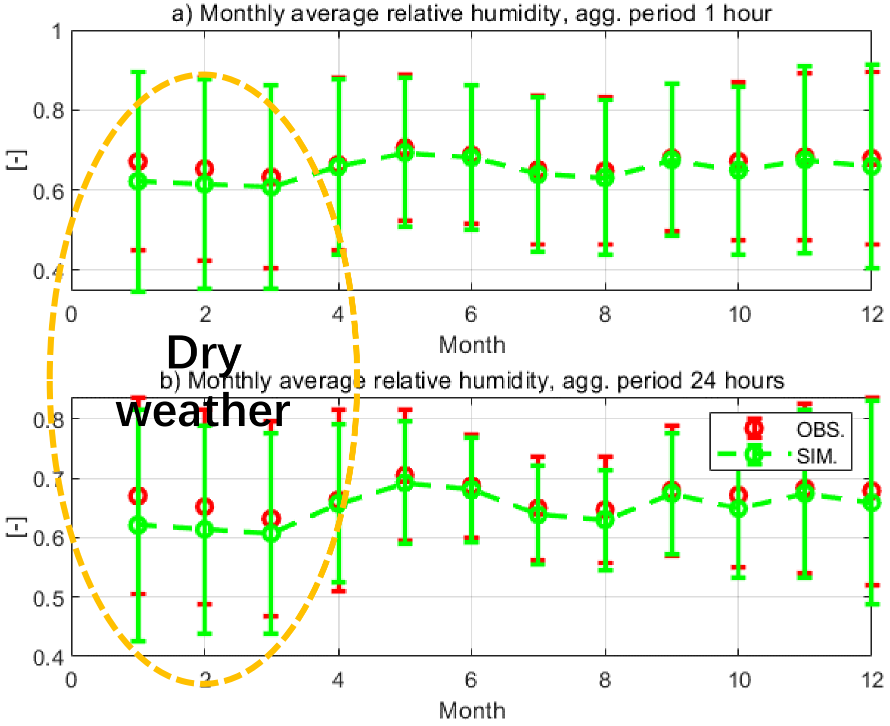

Fig.7.1 Comparison between the observed (red) and simulated (green) mean monthly **relative humidity** for aggregation periods of 1 hour (a) and 24 hours (b).

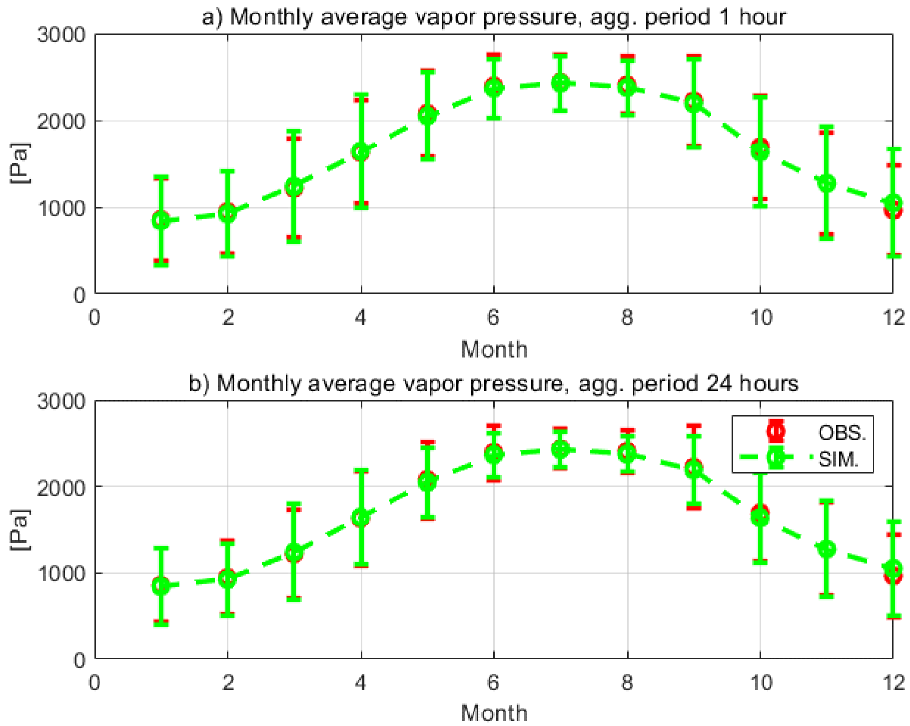

Fig.7.2 Comparison between the observed (red) and simulated (green) mean monthly **vapor pressure** for 1hr (a) and 24hrs (b) aggregation time periods.

Results and Analysis

➢ 5 Vapor Pressure

➢ Results analysis

1. Fig.7.3a) shows the model can capture the mean relative humidity in a daily cycle, and from the a good overlap during 8:00-19:00, that indicates a better match during day-time hours.
2. From the combination of Fig7.3a) and 7.4b), even that the daily trend of U can be simulated well, it is hard for model to capture the frequency of U, and it shows a nonlinear and irregular change, especially in the wet weather.
3. From the combination of Fig7.3b) and 7.4b), the distributions of e_a and U are rather frequent and shows non-linearities in the transformation. For greater e_a, that means a higher U leading to wet weather. However, it is hard to relate the simulation changing trend of wet or dry weather.
4. For the dew point temperature T_{dew}, when the air temperature is close to T_{dew}, the relative humidity approaches 1, indicating that the air is nearly saturated and storm may occur. In Fig.7.4a), there are obvious gaps between simulation and observation of T_{dew}, implying T_{dew} is simulated poorly.

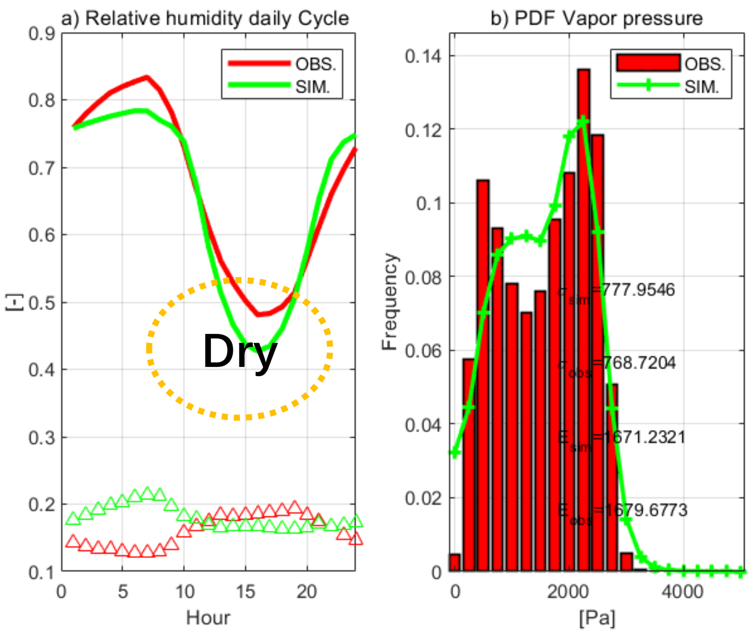

Fig.7.3 Comparison of relative humidity daily cycle (a) and vapor pressure probability density function (b).

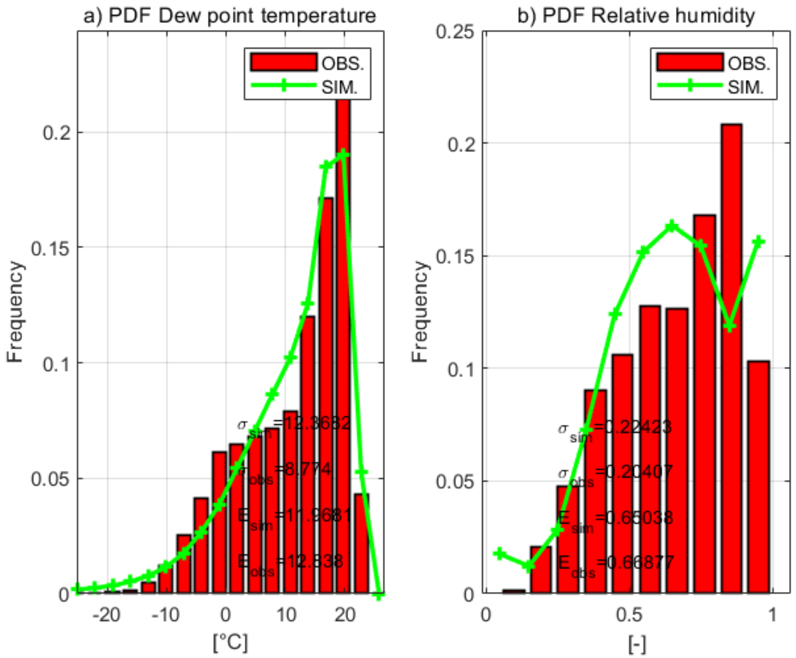

Fig.7.4 Comparison between the observed (red) and simulated (green) dew point temperature (a) and relative humidity (b) PFDs.

Results and Analysis

➢ 6 Wind Speed

➢ Results analysis

1. The probability density function of wind speed is well captured in AWE-GEN mostly (in Fig.8.1), except a lower speed. However, for these extreme wind conditions, like W_s>10m/s, the model cannot reproduce the observed speed.
2. In Fig.8.1b), without the extreme conditions, the wind speed daily cycle is reproduced correctly, especially at noon, the simulation wind speed almost overlaps with observation, and the distribution is approximating.

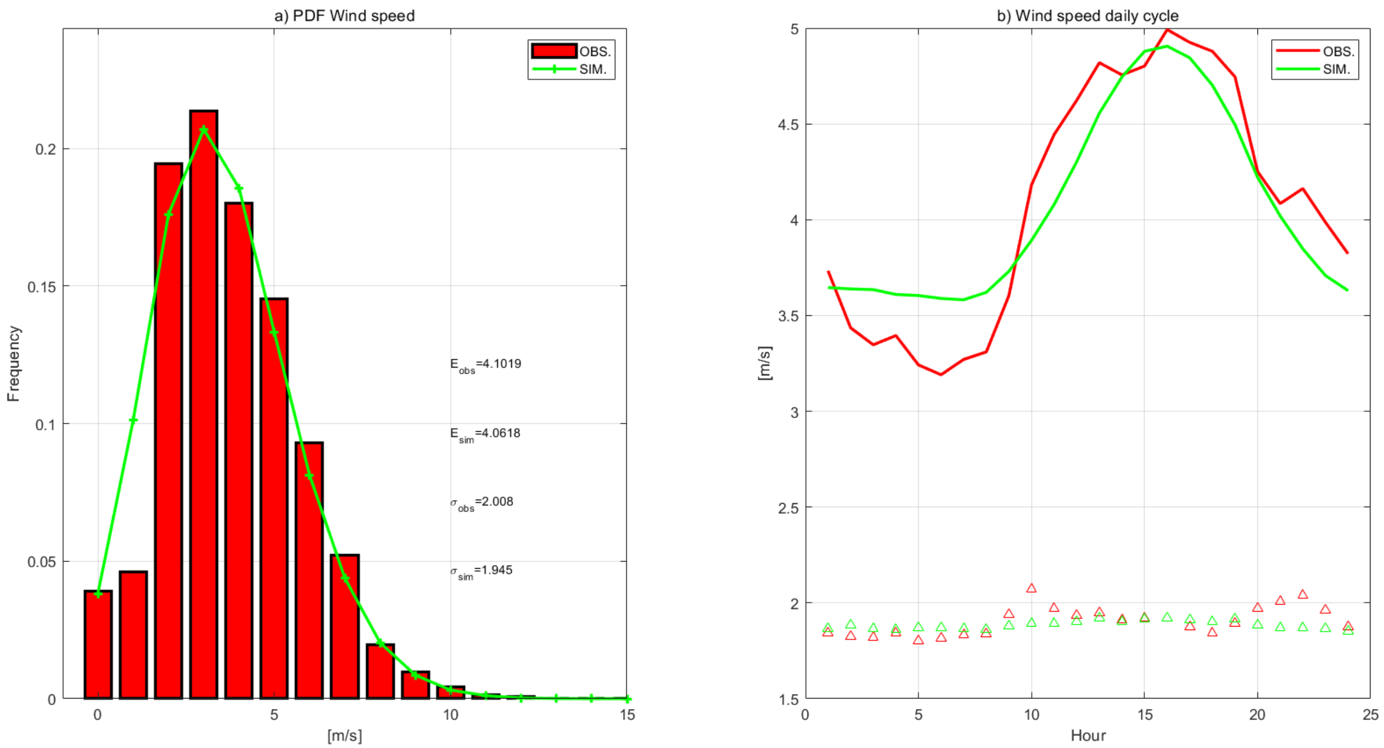

Fig.8.1 Comparison between the observed (red) and simulated (green) wind speed probability density function (a) and daily cycle of wind speed (b).

References

[1] 'AWE_GEN_v1.0_TECHNICAL_REFERENCE.pdf'.

[2] 'AWE-GEN - USER MANUAL.pdf'.

[3] A. H. Syafrina, A. Norzaida, and O. Noor Shazwani, 'Stochastic Modeling of Rainfall Series in Kelantan Using an Advanced Weather Generator', *Eng. Technol. Appl. Sci. Res.*, vol. 8, no. 1, pp. 2537–2541, Feb. 2018, doi: 10.48084/etasr.1709.

[4] C. W. Richardson, 'Stochastic simulation of daily precipitation, temperature, and solar radiation', *Water Resources Research*, vol. 17, no. 1, pp. 182–190, 1981, doi: 10.1029/WR017i001p00182.

[5] S. Fatichi, V. Y. Ivanov, and E. Caporali, 'Simulation of future climate scenarios with a weather generator', *Advances in Water Resources*, vol. 34, no. 4, pp. 448–467, Apr. 2011, doi: 10.1016/j.advwatres.2010.12.013.

[6] S. A. Halim, 'PROJECTIONS OF FUTURE EXTREME RAINFALL EVENTS USING STATISTICAL DOWNSCALING IN MALAYSIA'.

[7] A. H. Syafrina, M. D. Zalina, and L. Juneng, 'Future projections of extreme precipitation using Advanced Weather Generator (AWE-GEN) over Peninsular Malaysia', *Proceedings of IAHS*, vol. 364, pp. 106–111, Sep. 2014, doi: 10.5194/piahs-364-106-2014.

[8] N. Peleg, S. Fatichi, A. Paschalis, P. Molnar, and P. Burlando, 'From AWE-GEN to AWE-GEN-2d: a high spatial and temporal resolution weather generator', pp. EPSC2016-9330, Apr. 2016.

[9] M. Alves, D. F. Nadeau, B. Music, F. Anctil, and S. Fatichi, 'Can we replace observed forcing with weather generator in land surface modeling? Insights from long-term simulations at two contrasting boreal sites', *Theor Appl Climatol*, vol. 145, no. 1, pp. 215–244, Jul. 2021, doi: 10.1007/s00704-021-03615-y.

[10] C. Garijo and L. Mediero, 'Assessment of Changes in Annual Maximum Precipitations in the Iberian Peninsula under Climate Change', *Water*, vol. 11, no. 11, Art. no. 11, Nov. 2019, doi: 10.3390/w11112375.

[11] N. Peleg, P. Molnar, P. Burlando, and S. Fatichi, 'Exploring stochastic climate uncertainty in space and time using a gridded hourly weather generator', *Journal of Hydrology*, vol. 571, pp. 627–641, Apr. 2019, doi: 10.1016/j.jhydrol.2019.02.010.

Contribution Statement

1. Downloaded the data in SA, and ran 21 times AWE-GEN.
2. Read papers and organized the methodology for each climate variable, mainly from [1] and [6].
3. Coded in MATLAB for RMSE to analyse model performance, but it can be used in a small extent, like for precipitation comparison.
4. Read results figures from AWE-GEN model and interpreted the results.
5. Limited by capacity, some factors and results cannot be explained clearly.